

Dysregulation of miR-711 exerts a protective role against the X-ray-induced-injury in human umbilical vein endothelial cells

Z. Liu¹, Y. Wang², H. Xin³, Sh. Sun^{4*}

¹Department of Supply Room, Affiliated Hospital of Weifang Medical University, Shandong, 261041, China

²Medical Department, Affiliated Hospital of Weifang Medical University, Shandong, 261041, China

³School of Medical Imaging, Weifang Medical University, Shandong, 261053, China

⁴Vascular Interventional Surgery Department, Affiliated Hospital of Weifang Medical University, Shandong, 261041, China

ABSTRACT

► Original article

*Corresponding author:

Shunji Sun, Ph.D.,

E-mail:

shun8300duixu@163.com

Received: May 2022

Final revised: September 2022

Accepted: September 2022

Int. J. Radiat. Res., April 2023;
21(2): 325-330

DOI: 10.52547/ijrr.21.2.21

Keywords: miR-711, MAFG, HUVECs, X-ray, percentage of survival, apoptosis.

Background: Radiation therapy inevitably causes certain radiation damage to normal cells such as human vascular endothelial cells (HVECs), in addition to eliminating tumor cells. This article discusses the influence of miR-711 on the survival and apoptosis of human umbilical vein endothelial cells (HUVECs) after X-ray radiation. **Materials and Methods:** The expression of miR-711 and v-maf musculoaponeurotic fibrosarcoma oncogene family protein G (MAFG) was detected by real-time quantitative polymerase chain reaction (RT-qPCR), and the content of vascular cell adhesion molecule 1 (VCAM-1) in serum was detected by Enzyme-linked immunosorbent assay (ELISA). The survival and apoptosis of HUVECs after X-ray irradiation were analyzed by functional experiments, and validation of MAFG as a miR-711 target was done by dual-luciferase reporter assay. **Results:** In the serum of prostate cancer patients miR-711 was up-regulated, while MAFG was down-regulated compared to the control group. After X-ray radiation intervention, miR-711 levels were increased, in contrast, MAFG levels decreased with a concomitant increase in VCAM-1 expression. The percentage of survival level of HUVECs decreased gradually and the apoptosis rate of HUVECs increased as the dosage of X-ray radiation increased. Notably, after 2Gy X-ray radiation, the miR-711 inhibitor increased the survival rate of HUVECs while reducing the apoptosis rate, in contrast to the miR-711 mimic decreased the survival rate of HUVECs and increased the apoptosis. Besides, luciferase activity assay demonstrated the targeting of miR-711 to MAFG. **Conclusion:** The inhibition of miR-711 might abrogate the function of X-ray irradiation on the survival and apoptosis of HUVECs.

INTRODUCTION

Radiation therapy is a method of locally treating tumors using gamma rays, X-rays or electrons beams (1, 2), which is one of the medical applications of ionizing radiation (3). X-rays were the most widely used and fastest medical imaging method, discovered by Wilhelm Konrad Rontgen in 1895 (4). Studies have long demonstrated the application of X-rays in medical imaging and diagnostic therapy (5-7). Previous studies suggest that X-rays could be used for the treatment of prostate cancer (8,9). Therefore, prostate cancer patients were selected as the subjects in this study as X-ray radiation is used as a treatment option. The serum samples before and after X-ray radiation intervention were collected to further explore the significance of X-rays in disease treatment.

MicroRNAs (miRNAs) regulate gene expression by interfering with transcription, translation, or binding to the 3'untranslated region (3'UTR) base of a target

gene through complementary bases (10, 11). Ionizing radiation has been implicated to play a regulatory role in tumor radiation therapy by inducing the expression of certain miRNA (12). Mohammad and his colleagues believe that miR-711 may play a key role in prostate cancer progression by regulating cancer cell survival signaling cascades essential for cancer cell survival and serves as a biomarker for poor prognosis in prostate cancer (13). In addition, miR-711 is also implicated in the treatment of gastric cancer (14). There are also literatures stating that miR-711 can be used as a therapeutic target for many diseases such as Alzheimer's disease and traumatic brain injuries (15,16). However, the effect of the aberrant miR-711 expression on HUVECs post-X-ray radiation is unclear and requires detailed investigation.

In this paper, miR-711, MAFG and VCAM-1 expression in the serum of prostate cancer patients before and after radiotherapy were quantified and compared to understand the regulatory effect of

miR-711 on HUVECs. Moreover, the influences of X-ray intervention on the survival and apoptosis of HUVECs was investigated and luciferase activity analysis of the sponge relationship between miR-711 and MAFG. This provided a theoretical basis for radiation therapy of prostate cancer patients in the future.

MATERIALS AND METHODS

Radiotherapy patient information

For this study, we included 61 prostate patients and 42 healthy controls, totaling 103 subjects from the affiliated hospital of Weifang Medical University. Venous blood (3 ml) was collected from subjects, centrifuged at 1500 x g for 10 min at 4°C (High-speed refrigerated centrifuge; Eppendorf, Germany), and the serum was separated and stored in a -80 °C refrigerator (Haier, China) for later use.

Ionizing radiation

X-ray irradiation was performed using a 320 kV, 10 mA X-ray machine (North Branford, USA) with a 2 mm aluminum filter at dose rates of 0, 2, and 4 Gy/min.

Cell culture and transfection

HUVECs were selected as the cell line model for this assay and were obtained from the Cancer Manufacturers Research Center (Tumor Hospital, Chinese Academy of Medical Sciences, Beijing). HUVECs have stem cell-like potential and have been widely selected as an in vitro experimental model for the study of endothelial cell biology, and a variety of diseases^(17,18). HUVECs were cultured in RPMI 1640 medium (Gibco; Carlsbad, USA) with 10% fetal bovine serum (FBS; Carlsbad, USA).

Transfections in HUVECs were performed with miR-negative control (miR-NC), 2Gy, miR-711 mimic, and miR-711 inhibitor using Lipofectamine 3000 (Invitrogen, Shanghai) for 48 h. The miRNAs were synthesized by Thermo Fisher Scientific and the sequences are as follows: miR-711 mimic: 5'-GGGACCCAGGGAGAGACGUAAG-3'; miR-711 inhibitor: 5'-CUUACGUCUCUCCUGGGUCCC-3'.

RT-qPCR assay and ELISA detection assay

TRIzol (Invitrogen, USA) reagent was used to extract total RNA from serum and cell line samples. RNA was reverse transcribed into cDNA using the PrimeScript RT reagent kit (Takara, Japan). For real-time PCR, SYBR Green PCR kit (Takara, Japan) was used and the reaction was performed on Applied Biosystem 7500 real-time PCR system (USA). The fold change values were calculated by the established 2-ΔΔCt method. U6 (Invitrogen, USA) served as an internal reference control.

The content of VCAM-1 in the serum samples were determined after drawing a standard curve

under the guidance of the ELISA kit (Biosource International, USA).

Cell Counting Kit-8 (CCK-8) assay

HUVECs were seeded in 96-well plates at a seeding density of 3×10^3 cells/ml and cultured at 37°C for 12 h. Then they were randomly divided into three groups and received X-ray irradiation at dose rates of 0, 2, and 4 Gy/min. Post 72 hours of irradiation, 10 μl of CCK-8 reagent (Dojindo, Japan) was added to the wells. After incubating for another 2 h at 37°C, the absorbance was measured at 450 nm.

Cell apoptosis analysis

HUVECs were collected 48h after transfection, Annexin V-FITC kit (Invitrogen, USA) was used for staining. Post staining, the cells were analyzed by flow cytometry (Becton Dickinson, USA) and the Annexin V positive cells were quantified.

Bioinformatic analysis and dual-luciferase reporter assay

The potential target genes of miR-711 were predicted by StarBase v2.0 online program, and MAFG was identified as a potential target as it had a complementary sequence with miR-711. To verify whether MAFG directly targets miR-711, the MAFG sequence was used to construct WT-MAFG (wild-type) or MUT-MAFG (mutated-type). The WT-MAFG or MUT-MAFG constructs were co-transfected with miR-NC, miR-711 mimic, or miR-711 inhibitor using Lipofectamine 3000. Post 24 hours of transfection, the luciferase activity was evaluated via a luciferase detection kit (Promega, USA).

Statistical analysis

To ensure accuracy, each group was repeated at least 3 times, and all data were expressed as mean ± standard deviation. Differences between two groups were analyzed using Student's t-test, and a one-way analysis of variance (ANOVA) was performed for experiments involving more than two groups. Data were processed with the software SPSS 20.0 and Graphpad Prism 7.0 (CA, USA). $P < 0.05$ was considered statistically significant.

RESULTS

Subject clinical relevance

We found no statistical difference in age, BMI, smoking status, or drinking history ($P > 0.05$) between prostate cancer patients and healthy individuals in table 1.

The expression of miR-711, MAFG, and VCAM-1 in serum

We then assayed the levels of miR-711 and MAFG in the serum of prostate patients and healthy individuals using RT-qPCR. In Figure 1A, miR-711

was decreased in prostate patients compared to healthy individuals ($P < 0.001$). In contrast, MAFG was elevated in the serum of prostate patients ($P < 0.001$, figure 1B).

The content of VCAM-1 in serum was determined by ELISA detection assay. In figures 2A and 2B, the level of miR-711 was elevated in the serum of prostate patients after radiation, while the expression of MAFG was decreased ($P < 0.001$). The results of the ELISA assay in figure 2C suggested that the content of VCAM-1 in the serum markedly increased after radiation therapy ($P < 0.001$).

Effects of different doses of radiation on HUVECs

To understand the molecular mechanisms, we used in vitro cell culture using HUVECs. HUVECs were given X-ray radiation of 0Gy, 2Gy, and 4Gy respectively, and the results were as follows. The percentage of surviving cells gradually decreased with an increase in X-ray radiation dose (figure 3A; $P < 0.001$). It was speculated that high-dose X-ray radiation inhibited cells activity. In addition, the apoptosis rate of HUVECs increased after 2Gy X-ray radiation, with the maximum apoptosis rate of HUVECs observed after 4Gy X-ray radiation compared with the 0Gy group (figure 3B; $P < 0.001$). To avoid the excessive side-effects of X-rays radiation on HUVECs, this study selected a 2Gy X-ray radiation dose for the subsequent studies.

Effects of miR-711 on the survival and apoptosis of HUVECs

To understand the role of miR-711 on the

radiation-induced damage, miR-NC, miR-711 mimic, and miR-711 inhibitor were transfected into HUVECs, and the cells were exposed to 2Gy X-ray radiation. After 2Gy X-ray radiation, miR-711 mimic elevated the of miR-711 level in HUVECs, while the miR-711 inhibitor inhibited miR-711 expression (figure 4A). For figure 4B, the miR-711 inhibitor greatly increased the percentage of survival cells, whereas the miR-711 mimic suppressed the survival rate of HUVECs. Annexin V staining implied that miR-711 mimic enhanced the apoptosis rate of HUVECs, and the miR-711 inhibitor reduced the apoptosis rate (figure 4C). This suggested that the abnormal expression of miR-711 after 2Gy X-ray radiation might affect the survival of HUVECs.

Luciferase activity detection assay

Prediction analysis of miR-711 target genes revealed that miR-711 had complementary sequences with MAFG indicating potential binding in figure 5A. Luciferase gene detection assay indicated that in HUVECs transfected with WT-MAFG, the luciferase activities were decreased by miR-711 mimic, but they were increased by miR-711 inhibitor. However, transfection of MUT-MAFG did not markedly affect the luciferase activity ($P < 0.001$, figure 5B). Moreover, MAFG in HUVECs was detected by RT-qPCR. Figure 5C illustrated that miR-711 mimic decreased the level of MAFG, and an increased level of MAFG was observed when transfected with miR-711 inhibitor ($P < 0.001$). These results validate MAFG as a target of miR-711.

Table 1. Clinical data of the study population.

Variables	All subjects (N=103)		P value
	Healthy individuals (n=42)	Prostate Cancer (n=61)	
Age (years)	68.48±8.72	67.54±7.14	0.552
BMI (kg/m ²)	23.11±2.12	22.98±1.90	0.732
Smoking state			0.682
Yes	21	28	
No	21	33	
Drinking state			0.518
Yes	20	33	
No	22	28	
Gleason (n)			
≤7	-	56	-
>7	-	5	-
TNM stage (n)			
I-II	-	48	-
III-IV	-	13	-
Clinical stage (n)			
T1-T2	-	53	-
T3-T4	-	8	-

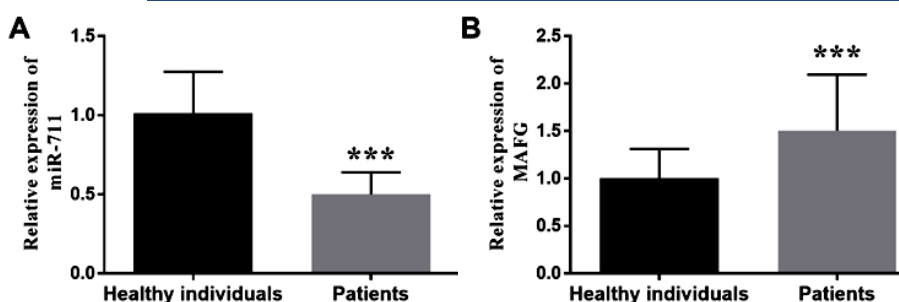


Figure 1. Expression levels of miR-711 and MAFG in serum of prostate patients. (A) miR-711 was down-regulated in the serum of prostate patients. (B) MAFG was up-regulated in the serum of prostate patients compared with healthy individuals. *** $P < 0.001$, in comparison with healthy individuals.

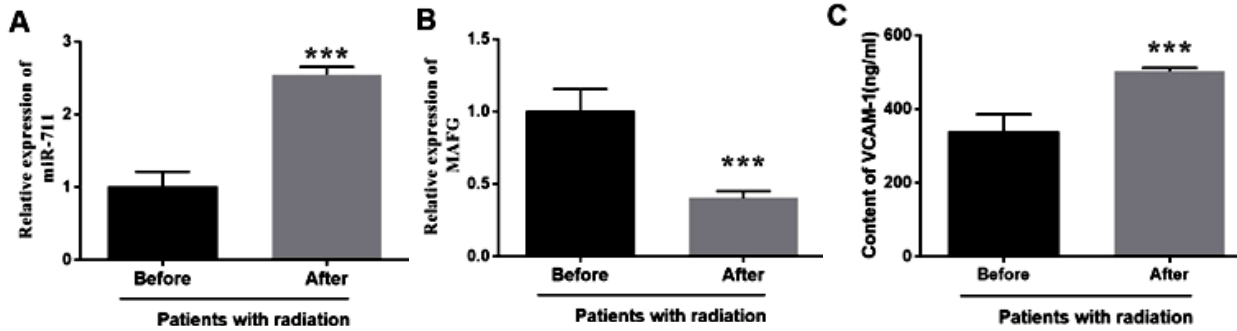


Figure 2. Serum levels of miR-711, MAFG, and VCAM-1 in prostate patients before and after X-ray radiation. (A) miR-711 was elevated after radiation in the serum of prostate patients. (B) MAFG expression in the serum of prostate patients decreased after radiation. (C) The content of VCAM-1 in the serum of prostate patients increased after radiation. ***P < 0.001, in comparison with before radiation.

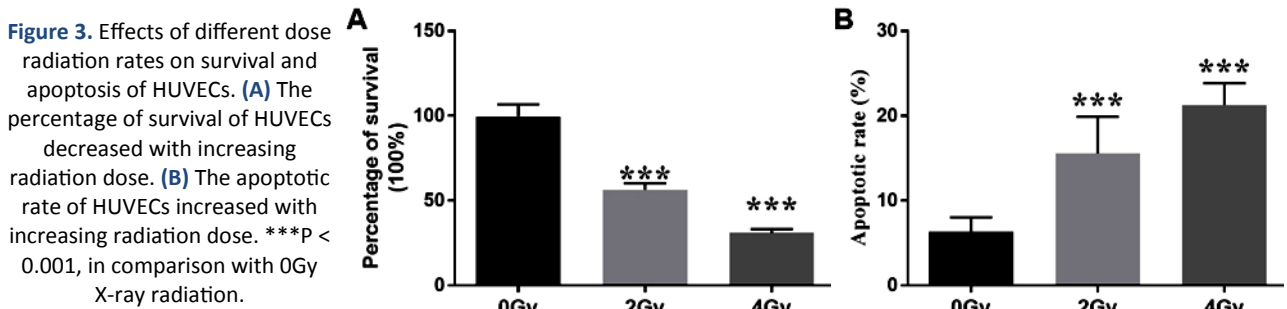


Figure 3. Effects of different dose radiation rates on survival and apoptosis of HUVECs. (A) The percentage of survival of HUVECs decreased with increasing radiation dose. (B) The apoptotic rate of HUVECs increased with increasing radiation dose. ***P < 0.001, in comparison with 0Gy X-ray radiation.

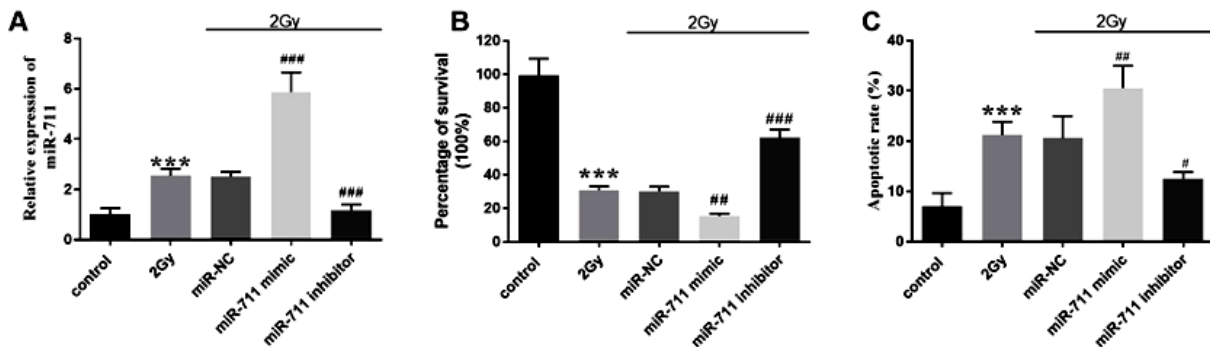


Figure 4. The effect of miR-711 on the survival and apoptosis of HUVECs after 2Gy X-ray radiation. (A) The influences of miR-711 mimic and inhibitor on miR-711 expression. (B) MiR-711 inhibitor enhanced the percentage of survival of HUVECs. (C) MiR-711 mimic increased the apoptotic rate of HUVECs. ***P < 0.001, in comparison with control; ####P < 0.001, ###P < 0.01, #P < 0.05, in comparison with 2Gy X-ray radiation.

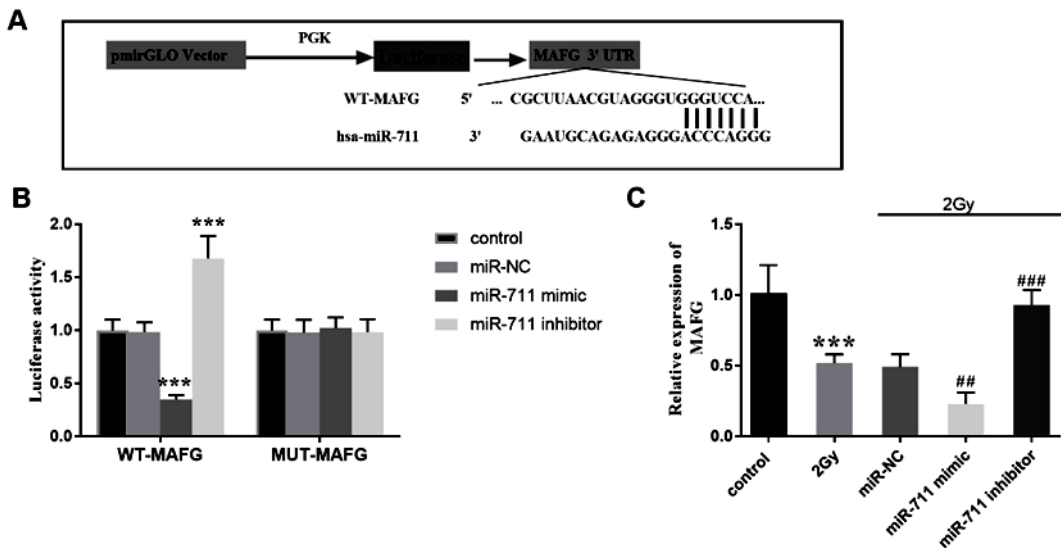


Figure 5. Luciferase gene report detection assays. (A) The predicted potential binding sites of miR-711 to MAFG. (B) The luciferase activities of WT-MAFG were reversely controlled by miR-711, rather than MUT-MAFG. (C) The effect of miR-711 on the relative expression of MAFG. ***P < 0.001, in comparison with control; ####P < 0.001, ###P < 0.01, in comparison with 2Gy X-ray radiation.

DISCUSSION

Ionizing radiation refers to rays with short wavelength, high frequency, and high energy, which find applications in medical and industrial fields (19). Radiation therapy is an application of ionizing radiation in the medical field that has been widely accepted as a treatment for cancer patients and has achieved remarkable results, controlling the prognosis of cancer patients (20). Studies have shown that proton radiation therapy, is a safe and effective method, and has a high therapeutic effect on prostate cancer (21). It has been shown that ZIF-82-PVP nanoparticles can effectively promote the apoptosis of hypoxic prostate cancer cells under X-ray irradiation thereby potentially improving the clinical outcome of radiation therapy (22). However, radiation therapy may cause cell DNA damage, and even induce tumors or genetic diseases in non-cancerous cells (23, 24). Moreover, radiation therapy may also cause vascular endothelial injury, decreased blood vessel density, fibrosis, and other consequences (25, 26). Therefore, in the context of prostate cancer research, it has certain theoretical significance to discuss the induction effect of X-ray.

With the advent of molecular biology in disease treatment, miRNAs have become attractive tools targets and can act as therapeutics for various diseases. It has been experimentally observed that miR-711 was significantly downregulated in prostate cancer tissues compared to the adjacent normal tissues, which corroborates our findings (13). MAFG is a MAF protein that has been identified as a receptor target (27). There are studies have demonstrated that MAFG is associated with the progression of liver and colorectal cancers (28, 29). The investigation of epithelial immunity revealed that functional manipulation of miR-218 caused changes in the expression of its predicted target MAFG, and the expression of MAFG was reduced by transfection of bronchial epithelial cells with miR-218 precursors [30]. Recent reports suggest that MAFG may be involved in the EIF3J-AS1 mediated malignant phenotype of prostate cancer cells, and MAFG was up regulated in tumors (31). MAFG is enhanced in the serum of prostate cancer patients, and post-X-ray radiation, miR-711 increased and MAFG decreased.

VCAM-1, known to be secreted by endothelial cells, is a typical adhesion molecule expressed in HUVECs and can modulate a variety of diseases (32-34). We found that VCAM-1 was increased in the serum of prostate patients after X-ray radiation. Haubner et al demonstrated that an increased in the X-ray radiation intensity was accompanied by a concomitant increase in VCAM-1 level in human dermal microvascular endothelial cells (HDMEC) (35), which is consistent with the results of this study. In the exploration to elucidate the mechanism of action of miR-711, we learned that unlike miR-711 mimic,

miR-711 inhibitor treatment contributed to the survival of cells and reduced the apoptosis rate. In the exploration of Sabirzhanov *et al.*, it was also stated that miR-711 inhibited the intrinsic apoptosis after attenuated irradiation (36). In other words, miR-711 suppressed the expression of HUVECs with higher vitality, which was more conducive to patient survival. Subsequent luciferase assays experimentally confirmed that miR-711 targeted MAFG, and miR-711 inhibitor treatment reversed the low expression of MAFG in HUVECs after X-ray radiation.

In conclusion, this study shows that X-ray radiation affects the levels of miR-711 in prostate cancer patients. We observed that the survival rate of HUVECs gradually decreased as the X-ray radiation dose was enhanced, and conversely the apoptosis rate gradually increased. After moderate X-ray radiation, therapeutic interventions such as miR-711 inhibitor could reverse the elevated miR-711 and down-regulate MAFG in the serum of patients thereby protecting the normal endothelium from radiation damage.

ACKNOWLEDGEMENTS

Not Applicable.

Ethics approval and consent to participate: This study had been approved by the Affiliated Hospital of Weifang Medical University. All patients have signed the informed consent.

Consent for publication: All patients have signed the informed consent.

Availability of data and materials: Available from the corresponding author.

Competing interests: The authors declare no conflict of interest.

Funding: There was no funding for this study.

Authors' contributions: All authors contributed to the study conception and design. Material preparation and data collection were performed by H X and S J S. Data analysis was conducted by Z Q L and Y W. The first draft of the manuscript was written by X H and all authors commented on previous versions of the manuscript. All authors read and approved the final manuscript.

REFERENCES

1. Wang X, Guo Z, Zhang C, Zhu S, Li L, Gu Z et al. (2020) Ultrasmall BiOI quantum dots with efficient renal clearance for enhanced radiotherapy of cancer. *Adv Sci (Weinh)*, **7**: 1902561.
2. Szatkowska M and Krupa R (2020) Regulation of DNA damage response and homologous recombination repair by microRNA in human cells exposed to ionizing radiation. *Cancers (Basel)*, **12**(7): 1838.
3. Nuszkiwicz J, Woźniak A, Szewczyk-Golec K (2020) Ionizing Radiation as a Source of Oxidative Stress-The Protective Role of Melatonin and Vitamin D. *Int J Mol Sci*, **21**(16): 5804.
4. Pfeiffer D, Pfeiffer F, Rummeny E (2020) Advanced X-ray Imaging Technology. *Recent Results Cancer Res*, **216**: 3-30.

5. Krishna AB, Tanveer A, Bhagirath PV, Gannepalli A (2020) Role of artificial intelligence in diagnostic oral pathology-A modern approach. *J Oral Maxillofac Pathol*, **24**: 152-6.
6. Elharrouss O, Subramanian N, Al-Maadeed S (2022) An Encoder-Decoder-Based Method for Segmentation of COVID-19 Lung Infection in CT Images. *SN Comput Sci*, **3**: 13.
7. Zhang X, Zhou J, Chai X, et al. (2018) The application of x-ray, computed tomography, and magnetic resonance imaging on 22 pediatric Langerhans cell histiocytosis patients with long bone involvement: A retrospective analysis. *Medicine (Baltimore)*, **97**: e0411.
8. Muzi M, O'Sullivan F, Perk T G, et al. (2021) Whole-body [(18)F]-fluoride PET SUV imaging to monitor response to dasatinib therapy in castration-resistant prostate cancer bone metastases: Secondary results from ACNRIN 6687. *Tomography*, **7**: 139-53.
9. Xie L, Zhang X, Chu C, et al. (2021) Preparation, toxicity reduction and radiation therapy application of gold nanorods. *J Nanobiotechnology*, **19**: 454.
10. Chen T, Xiao Q, Wang X, et al. (2019) miR-16 regulates proliferation and invasion of lung cancer cells via the ERK/MAPK signaling pathway by targeted inhibition of MAPK kinase 1 (MEK1). *J Int Med Res*, **47**: 5194-204.
11. Song H, Liu Y, Jin X, et al. (2019) Long non-coding RNA LINC01535 promotes cervical cancer progression via targeting the miR-214/EZH2 feedback loop. *J Cell Mol Med*, **23**: 6098-111.
12. Wagner-Ecker M, Schwager C, Wirkner U, et al. (2010) MicroRNA expression after ionizing radiation in human endothelial cells. *Radiat Oncol*, **5**: 25.
13. Waseem M, Ahmad MK, Srivastava VK, et al. (2017) Evaluation of miR-711 as novel biomarker in prostate cancer progression. *Asian Pac J Cancer Prev*, **18**: 2185-91.
14. Liao A, Tan G, Chen L, et al. (2016) RASSF1A inhibits gastric cancer cell proliferation by miR-711-mediated downregulation of CDK4 expression. *Oncotarget*, **7**: 5842-51.
15. Zhang Y, Xu C, Nan Y, Nan S (2020) Microglia-Derived Extracellular Vesicles Carrying miR-711 alleviate neurodegeneration in a murine Alzheimer's disease model by binding to itpkb. *Front Cell Dev Biol*, **8**: 566530.
16. Sabirzhanov B, Stoica BA, Zhao Z, et al. (2016) miR-711 upregulation induces neuronal cell death after traumatic brain injury. *Cell Death Differ*, **23**: 654-68.
17. Wan CX, Xu M, Huang SH, et al. (2018) Baicalein protects against endothelial cell injury by inhibiting the TLR4/NF- κ B signaling pathway. *Mol Med Rep*, **17**: 3085-91.
18. Baek JH, Kim K, Yang SS, et al. (2016) Preparation of extracellular matrix developed using porcine articular cartilage and *in-vitro* feasibility study of porcine articular cartilage as an anti-adhesive film. *Materials (Basel)* **9**(1): 49.
19. Siwek M and Edgecock T (2020) Application of electron beam water radiolysis for sewage sludge treatment-a review. *Environ Sci Pollut Res Int*, **27**: 42424-48.
20. Akomolafe IR and Chetty N (2021) Radioprotective potential of *Costus afer* against the radiation-induced hematological and histopathological damage in mice. *Radiat Oncol J*, **39**: 61-71.
21. Kamran SC, Light JO, Efstathiou JA (2019) Proton versus photon-based radiation therapy for prostate cancer: emerging evidence and considerations in the era of value-based cancer care. *Prostate Cancer Prostatic Dis*, **22**: 509-21.
22. Li Y, Gong T, Gao H, et al. (2021) ZIF-Based Nanoparticles Combine X-Ray-Induced Nitrosative Stress with Autophagy Management for Hypoxic Prostate Cancer Therapy. *Angew Chem Int Ed Engl*, **60**: 15472-81.
23. Chen Y, Gao H, Ye W (2018) Mitochondrial DNA mutations induced by carbon ions radiation: A preliminary study. *Dose Response*, **16**: 1559325818789842.
24. Emami Nejad A, Najafgholian S, Rostami A, Sistani A, Shojaeifar S, Esparvarinha M et al. (2021) The role of hypoxia in the tumor microenvironment and development of cancer stem cell: a novel approach to developing treatment. *Cancer Cell Int* **21**: 62.
25. Zhang P F, Wu J, Luo J H, et al. (2019) SNHG22 overexpression indicates poor prognosis and induces chemotherapy resistance via the miR-2467/Gal-1 signaling pathway in epithelial ovarian carcinoma. *Aging (Albany NY)*, **11**: 8204-16.
26. Stewart F A, Hoving S, Russell N S (2010) Vascular damage as an underlying mechanism of cardiac and cerebral toxicity in irradiated cancer patients. *Radiat Res*, **174**: 865-9.
27. Arnold P, Mojumder D, Detoledo J, et al. (2014) Pathophysiological processes in multiple sclerosis: focus on nuclear factor erythroid-2-related factor 2 and emerging pathways. *Clin Pharmacol*, **6**: 35-42.
28. (2014) MAFG mediates CIMP in BRAF-mutant colorectal cancer. *Cancer Discov*, **4**: Of11.
29. Liu T, Yang H, Fan W, et al. (2018) Mechanisms of MAFG dysregulation in cholestatic liver injury and development of liver cancer. *Gastroenterology*, **155**: 557-71.e14.
30. Liu J, Drescher KM, Chen XM (2009) MicroRNAs and Epithelial Immunity. *Int Rev Immunol*, **28**: 139-54.
31. Ye C, Qin S, Guo F, et al. (2022) LncRNA EIF3J-AS1 functions as an oncogene by regulating MAFG to promote prostate cancer progression. *J Cancer*, **13**: 146-52.
32. Dasgupta B, Chew T, deRoche A, Muller WA (2010) Blocking platelet/endothelial cell adhesion molecule 1 (PECAM) inhibits disease progression and prevents joint erosion in established collagen antibody-induced arthritis. *Exp Mol Pathol*, **88**: 210-5.
33. Zhang P, Hua L, Hou H, et al. (2018) Sphingomyelin synthase 2 promotes H2O2-induced endothelial dysfunction by activating the Wnt/ β -catenin signaling pathway. *Int J Mol Med*, **42**: 3344-54.
34. Luna C, Alique M, Naval Moral E, et al. (2016) Aging-associated oxidized albumin promotes cellular senescence and endothelial damage. *Clin Interv Aging*, **11**: 225-36.
35. Haubner F, Ohmann E, Pohl F, et al. (2013) Effects of radiation on the expression of adhesion molecules and cytokines in a static model of human dermal microvascular endothelial cells. *Clin Hemorheol Microcirc*, **54**: 371-9.
36. Sabirzhanov B, Makarevich O, Barrett J P, et al. (2020) Irradiation-Induced Upregulation of miR-711 Inhibits DNA Repair and Promotes Neurodegeneration Pathways. *Int J Mol Sci*, **21**(15): 5239.